Society for Mathematical Biology

ORIGINAL ARTICLE



Ribosome Abundance Control in Prokaryotes

Jacob Shea¹ · Lisa Davis¹ · Bright Quaye² · Tomas Gedeon¹

Received: 1 May 2023 / Accepted: 6 September 2023 © The Author(s), under exclusive licence to Society for Mathematical Biology 2023

Abstract

Cell growth is an essential phenotype of any unicellular organism and it crucially depends on precise control of protein synthesis. We construct a model of the feedback mechanisms that regulate abundance of ribosomes in *E. coli*, a prototypical prokaryotic organism. Since ribosomes are needed to produce more ribosomes, the model includes a positive feedback loop central to the control of cell growth. Our analysis of the model shows that there can be only two coexisting equilibrium states across all 23 parameters. This precludes the existence of hysteresis, suggesting that the ribosome abundance changes continuously with parameters. These states are related by a transcritical bifurcation, and we provide an analytic formula for parameters that admit either state.

Keywords Ribosome · Ribosome abundance control · Mathematical model

1 Introduction

Protein synthesis is a complex bio-polymerization process requiring significant commitment of cellular resources as well as precise regulation of hundreds of molecules. The two stages of protein synthesis, transcription and translation, form the crucial steps in the transfer of genetic information from DNA to protein. During the transcription process polymerases (RNAp) copy DNA-encoded genetic information to messenger

☐ Tomas Gedeon tgedeon@montana.edu

> Jacob Shea jacobshea406@gmail.com

Lisa Davis lisa.davis@montana.edu

Published online: 20 October 2023

Bright Quaye b.quaye@wustl.edu



Department of Mathematical Sciences, Montana State University, Bozeman, MT 59717, USA

Department of Economics, Washington University, St. Louis, MO, USA

119 Page 2 of 29 J. Shea et al.

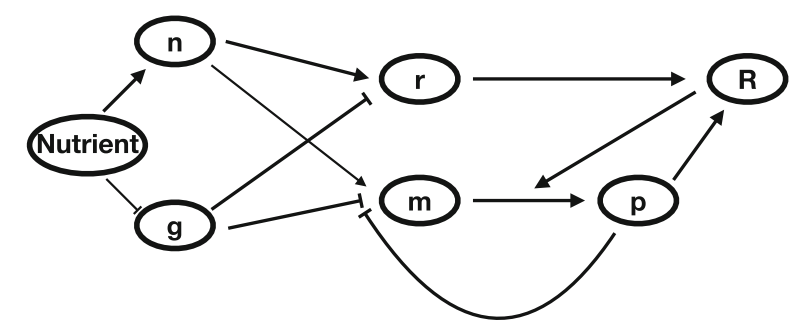


Fig. 1 Schematic description of the ribosome assembly control system. Ribosomes R are assembled from ribosomal RNA r and ribosomal proteins p, which are translated by ribosomes from mRNA m. Sufficient nutrient levels increase the pool of nucleotides n, which are building blocks of both rRNA and mRNA. Low nutrient levels cause a rise in ppGpp (g), which hinders rRNA and mRNA production. Free ribosomal proteins inhibit their own translation

mRNA. Translation is a similar process where ribosomes translate mRNA information into a polypeptide chain which subsequently folds to form a protein. In prokaryotes, both transcription and translation happen in the cytoplasm of a cell and can occur simultaneously. Therefore regulation of gene expression in bacteria, such as E. coli, primarily happens at the transcriptional level (Griffiths et al. 1999; Shaw 2008).

The control of bacterial growth rate centers around allocation of cellular resources (Klumpp and Hwa 2008; Erickson et al. 2017) to two fundamental activities—the construction of ribosomes vs. the production of all other proteins that the cell needs. There is a tight correlation between the growth rate and the fraction of RNA that is ribosomal RNA; when the growth rate is at its highest level, around 85% of all RNA is ribosomal RNA (Scott et al. 2010; Erickson et al. 2017; Scott et al. 2014; Weiße et al. 2015). On the other end of the spectrum, in sudden downshift of available resources, bacteria must quickly re-focus their resources from ribosome production and exponential growth to survival in the new environment. The response to such downshift is known as *stringent response* (Hauryliuk et al. 2015; Srivatsan and Wang 2008; Traxler et al. 2011; Boutte and Crosson 2013).

The translation process contains an important feedback loop: ribosomes are made up of proteins, which need to be translated by ribosomes. The goal of this paper is to develop a mathematical model of the main feedback loops that control abundance of ribosomes in response to external conditions, see Fig. 1. The model accounts for the concentrations of the free ribosomes R, ribosomal RNA (rRNA) denoted by r, and proteins p, which are translated from mRNA m using ribosomes R. We include direct negative feedback loops where ribosomal proteins, when in excess, slow down their own translation. The effect of a small signaling molecule guanosine tetra- and pentaphosphate, usually referred to as ppGpp, Hauryliuk et al. (2015), Ross et al. (2013), Ross et al. (2016), Boutte and Crosson (2013), is also included in the model and is denoted by g. The model also accounts for the effect of the abundance of building blocks for mRNA and rRNA synthesis n. We do not include in our model multiple constraints that restrict growth rate of the cell in a given environment. These include allocation of energy and ribosomes to production of transport proteins, enzymes and



ribosomes themseleves (Weiße et al. 2015; Scott et al. 2014). In particular, we focus on the central control loop that adjusts the number of ribosomes that translate ribosomal proteins in response to nutrient depletion and do not consider the allocation problem between ribosomes that translate enzymes and those that translate ribosomes (Scott et al. 2014). We will pursue incorporating the current model into the broader context of growth control in future work (Molenaar et al. 2009; Scott et al. 2014; Weiße et al. 2015). The focus of this work is the analysis of equilibrium states and the conditions that lead to transition between them.

The model consists of a system of six differential equations parameterized by 23 parameters. Our analysis shows that for all values of parameters, the system in (5) has either one equilibrium S, or two equilibria S and P in the biologically feasible region \mathbb{R}^{6+}

Equilibrium S represents the stationary state of the system where there are no free ribosomes, no free ribosomal proteins, and both the rRNA and mRNA concentrations remain at base level. In a broader context of allocation of cellular resources, this corresponds to a state of the cell where all existing ribosomes are engaged in translation. This is consistent with the observation that even at the lowest growth rates, a fraction of cellular proteome consists of ribosomes that are engaged in translation of housekeeping genes and ribosomal proteins. Therefore this state is consistent with a stationary growth phase.

The state P represents the proliferative state of the system where ribosomal proteins and ribosomes are being produced at a rate that results in ribosomes that are not needed for ribosomal protein translation. These extra ribosomes can be allocated to enzymes and transport complexes that allow cellular growth.

We show that P emerges from S by a transcritical bifurcation and, when P exists, it is asymptotically stable. When only the equilibrium S exists, it is also asymptotically stable. Since we cannot exclude existence of non-equilibrium dynamics in \mathbb{R}^{6+} , we cannot claim global convergence to either P or S in the parameter regimes when they are stable. However, numerical simulation results have only indicated convergence to one of these two equilibria.

Importantly, our results show that this system does not admit *hysteresis* between steady states. Such hysteresis would require bistability between two stable equilibria which in turn implies existence of a third equilibrium whose stable manifold separates their basin of attraction. There are no parameter sets that admit three equilibria.

The key determinant of the transition between the stationary regime (i.e when S is stable) and the proliferative regime (i.e when P is stable) is the state of the feedback loop between ribosomes and ribosomal proteins.

As shown in Theorem 1, the proliferative equilibrium P exists if and only if the production rate of ribosomal proteins exceeds a threshold value that is comprised of two terms. The first describes the demand for these proteins through production of ribosome rRNA scaffold, and the second terms describes the assembly rate of these proteins. Both of these terms are scaled by the product of the removal rates of proteins and mRNA.

The work identifies either parameter values or reasonable ranges for all 23 parameters, and we confirm existence of both stationary and proliferative states with the



119 Page 4 of 29 J. Shea et al.

ranges of these model parameters. Furthermore, the results show that eight (8) parameters do not significantly influence the transition between these states; four (4) model parameters do. These include nutrient availability I, which is a signal that the cell responds to by adjusting the number of ribosomes. In addition, this group includes the maximal transcription initiation rate for the rrn gene A_{max} , coding for rRNA, and the rate of ribosome assembly from mRNA and proteins α . The final parameter K = K(I) is proportional to parameter I as it reflects the size of amino acid pool which is proportional to the available nutrient.

2 Derivation of the System of Differential Equations

This section outlines the development of an ODE model of the system that controls the ribosome abundance in $E.\ coli$. Ribosomes contain around 50 ribosomal proteins organized around RNA scaffold (Condon et al. 1993, 1995; Gyorfy et al. 2015). The concentration of ribosomal proteins is represented by p, and the concentration of free ribosomes by R. Ribosomal proteins are translated from ribosomal protein mRNA. The concentration of free ribosomal protein mRNA is denoted by m. Ribosome production is controlled by the number of available rRNA scaffolds that are transcribed from an rrn gene; their concentration will be denoted by r. We assume that the rate of production of R from combining rRNA scaffold and ribosomal proteins p is α ; we simplify the model by assuming that this process has stochiometry 1; that is one unit of p binds one rRNA scaffold rather than considering all 50 different ribosomal proteins. In other words, p represents the concentration of a prototypical ribosomal protein.

Ribosomal proteins have high affinity to RNA scaffold and lower affinity to their own mRNA; as a result, when RNA scaffolds are limiting, ribosomal proteins will bind to their own mRNA, which prevents its translation, thereby down-regulating their own production via translation inhibition. This negative feedback loop assures that the number of ribosomal proteins closely matches the number of available scaffolds. We model this process as a chemical reaction

$$m + p \stackrel{k_1}{\rightleftharpoons} C$$

where, as above, m is the concentration of the free ribosomal protein mRNA and C is an inactive complex. In addition, we take into account a conservation law $m+C=m_0$ where m_0 is the total mRNA. Assuming equilibration of this reaction is much faster than the rate of change of both total mRNA m_0 and the total protein concentration p, we obtain the relationship $C = \frac{k_1}{k-1}mp$. Inserting this into the conservation law leads to

$$m = \frac{m_0}{1 + k_d p} = \frac{\frac{m_0}{k_d}}{\frac{1}{k_d} + p} =: \frac{m_0 \kappa}{\kappa + p},\tag{1}$$

where we used $k_d = \frac{k_1}{k_{-1}}$ and $\kappa := \frac{1}{k_d}$. The rate of change of the total mRNA m_0 is occurring on a slower time scale than the deactivation reaction. Since we do not



explicitly model the elongation process in this work, we equate the rate of change of the total number of mRNA to the initiation rate of mRNA transcription \hat{B}

$$\dot{m}_0 = \hat{B}i_m$$

where i_m is the concentration of the gene from which mRNA is transcribed. Due to the differences in expected lifespan of ribosomal proteins and mRNA (Milo and Phillips 2016) (BNID 106869,108404), it is reasonable to assume that p is changing on a slower time scale than m_0 . Differentiating (1) and assuming the \dot{p} term is negligible leads to the approximation

$$\dot{m} = \dot{m}_0 \frac{\kappa}{\kappa + p} - \frac{m_0 \kappa}{(\kappa + p)^2} \dot{p} \approx \dot{m}_0 \frac{\kappa}{\kappa + p}.$$

Therefore we will model the rate of production of free ribosomal protein mRNA by the differential equation

$$\dot{m} = \frac{\hat{B}\kappa i_m}{\kappa + p}.$$

An important control of the number of ribosomes in *E. coli* is the initiation rate of the rrn transcription. There are two main mechanisms of this control which we include in our model. First is the availability of nucleoside triphosphate (NTP) which is the building block of both rRNA and mRNA, and we include the concentration of free NTP, n, in the model. The second is a small signaling molecule ppGpp, whose concentration is denoted by g. Both of these signals report on the nutritional state of the cell (Murray et al. 2003). Concentrations of ppGpp and NTP regulate rRNA synthesis primarily at the level of transcription initiation (reviewed in Paul et al. 2004). In particular, rrn promoters are strongly inhibited when NTP concentrations are low, such as when cells are starved for nutrients or during the transition to stationary phase (Murray et al. 2003; Gaal et al. 1997; Paul et al. 2004). Therefore the initiation rates $\hat{A} = \hat{A}(n, g)$ and $\hat{B} = \hat{B}(n, g)$ of both rrn and mRNA respectively are increasing functions of n, see (7) and (8). The abundance of n is modeled by

$$\dot{n} = I - \gamma n(\hat{A} + \hat{B}). \tag{2}$$

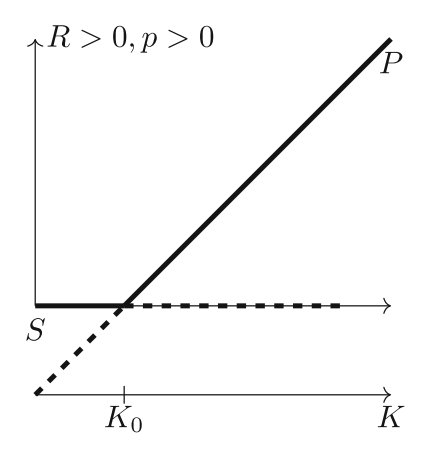
Here I represents the rate of nucleotide production in the cell, which is proportional to the rate of nutrient supply to the cell. One could assume this rate is time dependent, but for the current analysis, it is insightful to treat it as a parameter of interest. Therefore we interpret the parameter I as a proxy for the available nutrient supply to the cell. The second term is consumption of nucleotides during transcription of r and m, and γ is rate of incorporation of n into the rRNA and mRNA, respectively during both initiation and elongation.

The transcription initiation rate is affected both directly and indirectly by the concentration of ppGpp in the system. The indirect affect involves the presence of significant numbers of uncharged tRNA molecules. A *charged* tRNA is a tRNA molecule



119 Page 6 of 29 J. Shea et al.

Fig. 2 Bifurcation diagram illustrating Theorem 1. Boundary equilbrium S exists for all values of parameter K, but looses stability for $K > K_0$ when the stable equilibrium P enters the positive orthant R^{6+}



which has an attached amino acid. When the tRNA molecule transfers the amino acid to the polypeptide chain, the tRNA molecule loses that amino acid and must be *recharged* with a new amino acid (Brackley et al. 2010). In *E. coli* as well as in other bacteria, the presence of uncharged tRNAs that try to enter the ribosome is detected as a signal of slowing growth. In particular, a pair of enzymes RelA and SpoT, that are present at the ribosome, catalyze ppGpp in response to the presence of uncharged tRNAs (Hauryliuk et al. 2015; Srivatsan and Wang 2008; Traxler et al. 2011; Boutte and Crosson 2013).

In the most important direct effect, ppGpp binds directly to RNAp at two separate sites (Ross et al. 2013, 2016), and this binding destabilizes the open complex formation of those RNAps that transcribe the rrn gene (Hauryliuk et al. 2015; Srivatsan and Wang 2008). This leads to a lower initiation rate of the rrn gene; hence, in Fig. 2, the initiation rates of both mRNA and rRNA is reduced by the ppGpp binding. We model this effect by multiplying initiation rates \hat{A} and \hat{B} by a decreasing function of g, see (7) and (8). To model the production rate of g, we assume that g is produced when the available nutrient I(t) falls below a reference nutrient level, I_0 , that corresponds to the level required for sustained replication. This rate is then

$$H := -\min(I - I_0, 0).$$

We assume that the decay rate of g is η which results in

$$\dot{g} = H - \eta g \tag{3}$$

To model production of ribosomal proteins we assume that m and R bind first and this complex e := [mR] acts as an enzyme that transforms the substrate U of amino acids into protein p. The binding of m and R is governed by the reaction

$$m + R \stackrel{k_3}{\underset{k_{-3}}{\rightleftharpoons}} e$$



which equilibrates at

$$e = \frac{k_3}{k_{-3}} mR =: \hat{a}mR. \tag{4}$$

We note that \hat{a} has units of $(\mu M)^{-1}$.

The enzymatic reaction that turns amino acids into protein and is catalyzed by e = mR has a form

$$e + U \stackrel{k_1}{\underset{k_{-1}}{\rightleftharpoons}} C \stackrel{k_2}{\rightarrow} p + e$$

We assume that the forward reaction creating the complex C has the rate k_1 , while the backward rate is k_{-1} , which correspond to initial reversible binding of tRNA to ribosomes (Whitford et al. 2010). The second reaction creating p and e from the complex is irreversible and has rate k_2 . This represents the rate at which a representative ribosomal protein is produced.

We assume that the overall amount of enzyme stays constant $e_0 := \hat{a}mR$ on the time scale where protein translation takes place. Then the standard Michealis-Menten derivation (Michaelis and Menten 1913; Keener and Sneyd 2008) gives

$$K_m = \frac{k_{-1} + k_2}{k_1}$$
$$\dot{p} = e_0 \frac{k_2 U}{K_m + U}$$

Translating this into our problem where $e_0 = \hat{a}mR$ (see Eq. (4)), the rate of production of p is

$$\dot{p} = k_2 \hat{a} m R \frac{U}{K_m + U}.$$

Here k_2 has units of s^{-1} , \hat{a} has units μM^{-1} , both m, R are in μM and the ratio $\frac{U}{K_m+U}$ is dimensionless. The supply of amino acids U scales with the nutrient supply I to the cell $U = qI + I_1$, for some $I_1 < I_0$. However, the proportionality constant q depends in complex ways on the growth rate, environmental stress (Zampieri et al. 2019), pH values (Gale and Epps 1942) and the amino acid pool is under tight control (Elf and Ehrenberg 2005). We therefore do not impose a precise numerical relationship between U and I, but only impose this constraint at the end of the analysis.

On a longer time scale the population level of the enzyme e_0 is not constant. We assume that the initiation rate for translation is ω . Since the ribosomes are removed from the free pool when they bind mRNA, we include the term $-\omega \hat{a}mR$ in the ODE describing the rate of change of R. On the other hand, there are usually multiple ribosomes translating the same mRNA. Therefore we remove m from the pool of mRNAs at the rate $-\hat{\omega}\hat{a}mR$ where $\hat{\omega} := \frac{\omega}{\ell}$ with ℓ an average number of ribosomes on ribosomal protein mRNA.



119 Page 8 of 29 J. Shea et al.

The units of ω and $\hat{\omega}$ are s^{-1} . Finally, we assume that the decay rate of proteins is ξ , while the decay rate of rRNA and mRNA is β . We note that in the microbial growth experiments ξ usually represents growth rate of the cell population which dilutes the concentration of the protein. We arrive at the final model of the form

$$\begin{split} \dot{R} &= \alpha r p - \omega \hat{a} m R - \xi R \\ \dot{p} &= k_2 \hat{a} m R \frac{qI}{(K_m + qI)} - \alpha r p - \xi p \\ \dot{r} &= \hat{A} i_r - \alpha r p - \beta r \\ \dot{m} &= \frac{\hat{B} \kappa i_m}{\kappa + p} - \hat{\omega} \hat{a} m R - \beta m \\ \dot{n} &= I - \gamma n (\hat{A} + \hat{B}) \\ \dot{g} &= H - \eta g \end{split} \tag{5}$$

where i_r , i_m are concentration of the rrn and the ribosomal genes, respectively and

$$H = -min(I - I_0, 0)$$

$$\hat{A} = \hat{A}(n, g) = \left(A_2 \frac{n}{\kappa_1 + n} + A_1\right) \frac{\kappa_2}{\kappa_2 + g}$$

$$\hat{B} = \hat{B}(n, g) = \left(B_2 \frac{n}{\kappa_3 + n} + B_1\right) \frac{\kappa_4}{\kappa_4 + g}$$
(6)

We simplify the last two equations by combining parameters $A_{max} := A_2 \kappa_2$, $A_0 := A_1 \kappa_2$, $B_{max} := B_2 \kappa_4$, $B_0 := B_1 \kappa_4$ to get

$$\hat{A} = \hat{A}(n,g) = \left(A_{max} \frac{n}{\kappa_1 + n} + A_0\right) \frac{1}{\kappa_2 + g} \tag{7}$$

$$\hat{B} = \hat{B}(n, g) = \left(B_{max} \frac{n}{\kappa_3 + n} + B_0\right) \frac{1}{\kappa_4 + g}.$$
 (8)

After making the following substitutions

$$E(I) := \frac{qI}{K_m + qI}, \qquad G := \omega \hat{a}, \qquad K(I) := \frac{k_2}{\omega} E(I)$$

$$A := \hat{A}i_r \qquad B := \hat{B}\kappa i_m, \qquad f(p) := \frac{B}{\kappa + p} \tag{9}$$

the system of ODEs above in Eq. (5) simplifies to

$$\dot{R} = \alpha r p - G m R - \xi R \tag{10}$$

$$\dot{p} = KGmR - \alpha rp - \xi p \tag{11}$$

$$\dot{r} = A - \alpha r p - \beta r \tag{12}$$



$$\dot{m} = f(p) - \frac{G}{\ell} mR - \beta m \tag{13}$$

$$\dot{n} = I - \gamma n(\hat{A} + \hat{B}) \tag{14}$$

$$\dot{g} = H - \eta g \tag{15}$$

where \hat{A} , \hat{B} are defined in (7), (8), respectively.

The system (10)–(15) depends on 23 parameters, many of which either cannot be directly measured, or have not been measured to our present knowledge. Our goal is to make qualitative statements about all parameters. Since all parameters are nonnegative, we define a parameter space as the positive orthant $\mathcal{P} := \mathbb{R}^{23+}$, and we use $s \in \mathcal{P}$ to denote a vector of parameters in \mathcal{P} . As we will see next, the behavior of the system qualitatively depends on only three groups of parameters.

Theorem 1 Let A^* and B^* denote steady state levels of A and B in (9), which we explicitly compute in Sect. 4.1, and let

$$X := \alpha A^* \quad \epsilon := \xi \beta, \quad Z := GB^*$$

be groups of parameters. Let

$$K_0 := \left(1 + \frac{\epsilon}{X}\right) \left(1 + \kappa \frac{\epsilon}{Z}\right). \tag{16}$$

Then

if

$$K(I) < K_0$$

then $S = (0, 0, m_0, r_0, n^*, g^*)$ is the only equilibrium in \mathbb{R}^{6+} , and it is locally asymptotically stable;

if

$$K(I) > K_0$$

then S is unstable, and there is a unique equilibrium $P \in \operatorname{int} \mathbb{R}^{6+}$, $P = (R^{\dagger}, p^{\dagger}, m^{\dagger}, r^{\dagger}, n^{*}, g^{*})$. If there are no non-equilibrium invariant sets in $\operatorname{int} \mathbb{R}^{6+}$, then P is attracting all solutions in $\operatorname{int} \mathbb{R}^{6+}$.

Recall from Sect. 1 that the equilibrium *S* represents a *stationary state* when the cell does not have any free ribosomes in addition to those engaged in ribsomal protein translation. The equilibrium *P* represents a *proliferative state* where there are free ribosomes present in the cell that are available for translation of enzymes that can mediate biomass growth.

We now proceed with parameterization of the model and investigating those parameters which lead to states (phenotypes) represented by the equilibrium S and the equilibrium P.



119 Page 10 of 29 J. Shea et al.

3 Results

Note that Theorem 1 shows that the state of the system depends on four groups of parameters. They are

- $K(I) = \frac{k_2}{\omega} E(I)$ is the ratio of the ribosomal protein production rate and initiation rate of ribosomal mRNA-ribosome complexes multiplied by the supply level E(I) of amino acids, which is proportional to nutrient supply I to the cell.
- $X = \alpha A^*$ which is a product of rRNA production A^* and rate of assembly of rRNA into ribosomes α . Therefore X represents demand for ribosomal proteins imposed by supply rate of rRNA scaffold.
- $Z = GB^*$ is product of mRNA supply B^* and its assembly rate into ribosomal proteins G. Therefore Z represents the assembly rate of ribosomal proteins.
- $\epsilon = \xi \beta$ is a product of protein decay (dilution) rate ξ , and mRNA decay rate β .

In order to gain insight into the role of these constants, note that $\frac{\epsilon}{X}$ is the decay of ribosomal components divided by the demand for ribosomal proteins and $\frac{\epsilon}{Z}$ is the decay rate of ribosomal components divided by the assembly rate of ribosomal proteins. In order for the equilibrium P to exist, the value of K must be above the threshold value $K_0 = (1 + \frac{\epsilon}{X})(1 + \kappa \frac{\epsilon}{Z})$. When the decay rates are small the value of the threshold K_0 is small and it is easier for K to exceed the demand for ribosomal protein imposed by ribosomal assembly and satisfy $K > K_0$.

Our second level of model analysis uses values of biological parameters. Note that it is not a priori clear that within biologically feasible ranges of parameters both states S and P occur. We show not only that this is the case, but that the parameters that are implicated in transition from P to S indeed cause this transition when moved to lower limits of their ranges. We also show that there are many parameters that affect this transition very weakly, if at all. We have parameterized the model using information from existing literature on E. coli. The model contains 23 parameters, and we have identified values for 10 of them in the literature. The description of these 10 parameter values are in group 1 of Table 1. For the remaining 13 parameters, we identified reasonable parameter ranges for their values and listed those in Table 1. A detailed justification and list of references for the parameter values and their ranges can be found in Appendix A.

Analysis of the threshold K_0 from Theorem 1 shows that only the second term depends on κ . Using (9), we write

$$\kappa \frac{\epsilon}{Z} = \kappa \frac{\epsilon}{GB^*} = \kappa \frac{\epsilon}{G\hat{B}^* \kappa i_m} = \frac{\epsilon}{G\hat{B}^* i_m},$$

which shows that K_0 does not depend on the parameter κ . For this reason, we have separated κ from all three groups, and it is included in a separate first line of Table 1. Our goal is to explore the parameter ranges of the remaining 12 parameters in groups 2 and 3 of Table 1 and to determine how choices of these parameters result either in state S or in state P.

We begin by setting all 12 parameters to the value in the middle of their ranges, and we then classify the equilibrium. For this case, we found the proliferative equilibrium



Table 1 Values and ranges of values for the model parameters

	,	•	
Parameter K	Units µM	Value/range [11.29–119.56]	Interpretation Michealis-Menten constant for protein repression
Group I parameters			
β	s^{-1}	0.00233	Degradation rate of mRNA and rRNA
w	s^{-1}	0.000233	Protein degradation (dilution) rate
7	Unitless	1100	Nucleotides incorporated per initiation
U	μM	1.3	Amino acid average concentration
K_m	μМ	0.5	MM constant for protein production
I_0	$\mu M/s$	6212	NTP required for balanced growth
i_r	μM	0.01162	Concentration of rm genes
i_m	μМ	0.09133	Concentration of ribosomal protein genes
B_0	s-1	0	Minimal transcription initiation rate for mRNA
A_0	s^{-1}	0	Minimal transcription initiation rate for rrn
в	Unitless	5.14	Average number of ribosomes on mRNA
Group 2 parameters			
μ	s-1	[0.0033, 0.0058]	Degradation of ppGpp
$\boldsymbol{\beta}$	s_1	[0.33,2.64]	Rate of mRNA-ribosome complex formation
κ_1, κ_3	μM	$[10^3, 10^4]$	Half-saturation for NTP limitation
B_2	s–1	[1,3]	Maximal transcription initiation rate for mRNA times κ_2
\hat{a}	$(\mu M)^{-1}$	[2.33,18.52]	$\frac{1}{K_D}$ where K_D is dissociation constant for ribosomes binding to ribosomal mRNA
k_2		[1.05, 27.18]	K_{cat} for enzymatic reaction producing ribosomal proteins
Group 3 parameters			
I	$\mu M/s$	Free parameter	Nutrient availability
A_2	s-1	[0.46,6.76]	Maximal transcription initiation rate for rrn times κ_4
K2, K4	μM	[30,113]	Half-saturation for ppGpp repression. Here $\kappa_2 = \kappa_4$
α	$(\mu Ms)^{-1}$	[0.007,0.754]	Rate of ribosome assembly from rRNA and proteins
K(I)	Unitless	[0, 10.295]	Ratio of ribosomal protein production rate and its mRNA initiation rate times amino acid supply
The values of the nars	ameters in oronn 1 are	fixed throughout this work Th	The values of the narameters in oroun are fixed throughout this work. The narameters in oroun 2 affect the proliferative vs. stationary state weakly while the four narameters.

The values of the parameters in group 1 are fixed throughout this work. The parameters in group 2 affect the proliferative vs. stationary state weakly while the four parameters in group 3 have a strong impact on the state of the system



P. On the other hand, when all parameters are set to their lowest value of the range, we find equilibrium S. This demonstrates that the model is capable of capturing the range of predicted phenotypes over the reasonable biological range for the parameter values.

Next we examine the effect of the 5 parameters in group 3 of Table 1. Our analysis shows that changes in these parameters most directly influence the transition from the proliferative equilibrium P to stationary equilibrium S. These parameters denote the nutrient availability I, maximal transcription initiation rate for the rrn gene A_{max} , the rate of ribosome assembly α and K, the ratio of ribosomal protein production rate and its mRNA initiation rate. Lastly, two of these parameters, κ_2 and κ_4 , represent half-saturation constants of the effect of ppGpp on initiation rates of rrn and mRNA for ribosomal proteins. In the absence of information that these effects are significantly different, we assume $\kappa_2 = \kappa_4$ for the results of numerical simulations presented here; however, we treat them as distinct in the mathematical analysis of Sect. 4.1.

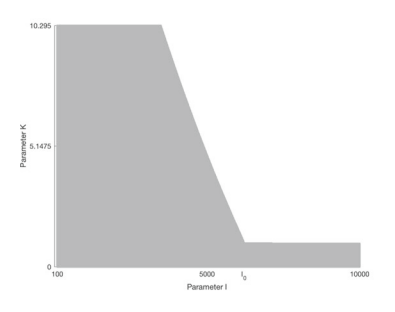
We fix the remaining 7 parameters in group 2 of Table 1 at the bottom of their ranges. We then investigate the five dimensional parameter space formed by those parameters in group 3 $(I, A_{max}, \alpha, K, \kappa_2 = \kappa_4)$ by selecting 200 samples from each range and classifying them, using Theorem 1, as admitting either the S or P equilibrium state. To visualize this space we fix values of A_{max} , α and κ_2 at either their low, or middle of their range values and vary the parameters K and I within their ranges, remembering that K is proportional to I. On these two dimensional projections of the five dimensional parameter space we indicate the phenotype by a color as a function of the remaining two parameters. The pair of parameter values that admit a stationary equilibrium S are grey, while points where the pair of parameters admit proliferative equilibrium P are white. In all panels in Fig. 3 the value of κ_2 is low, while in all panels in Fig. 4 the value of κ_2 is in the middle of its interval. In both figures, Panel (C) represents the situation where A_{max} and α are at the bottom of their ranges, while Panel (B) represents the situation where A_{max} and α are in the middle of their ranges.

We now apply our modeling assumption that K = K(I) is proportional to nutrient supply I, but that the proportionality constant depends in a complex way on factors like growth rate, pH and environmental stresses. In spite of this uncertainty, the panels allow us to make qualitative conclusions. Note that for any proportionality constant v in K = vI, the parameters (K, I) form a line with positive slope. We can conclude that for the transition from proliferative equilibrium P to stationary equilibrium S to occur, at least one of the values A_{max} and α must fall towards the lower limit of their range, and the value of I must be below $I = I_0$.

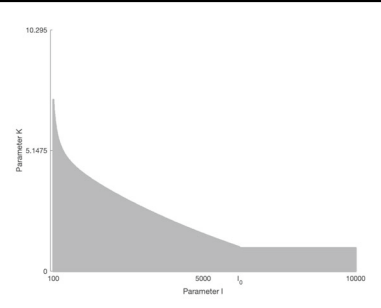
Note that nutrient availability I represents a signal that the cell responds to by adjusting the number of ribosomes, while both maximal transcription initiation rate for rrn gene, A_{max} (Griffiths et al. 1999; Shaw 2008), and the rate of ribosome assembly from mRNA and proteins, have been implicated as control points for ribosome abundance. Therefore the sensitive parameters agree with putative control points of the real system.

We now examine how the values of the seven parameters from group 2 in Table 1 that are fixed at the bottom of their intervals in Figs. 3 and 4 impact the prevalence of *S* vs. *P*. To achieve this, we assign all eight parameter values to the middle of their range (see Fig. 5E–H) and compare these to the graphs in the Figs. 3, and 4 parts

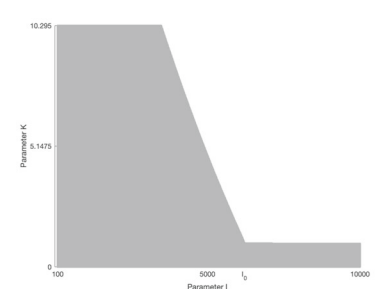




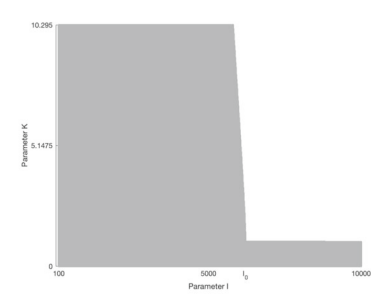
(A) Parameters $\kappa_2, \kappa_4 = 30$ and $A_2 = 0.46$ are at the bottom of their ranges, while $\alpha = 0.3805$ is in the middle of its range.



(B) Parameter κ_2 , $\kappa_4 = 30$ is at the bottom of its range, while parameters $A_2 = 3.61$ and $\alpha = 0.3805$ are in the middle of their ranges.



(C) All parameters κ_2 , $\kappa_4 = 30$, $A_2 = 0.46$, and $\alpha = 0.007$ are prescribed at the bottom of their ranges.



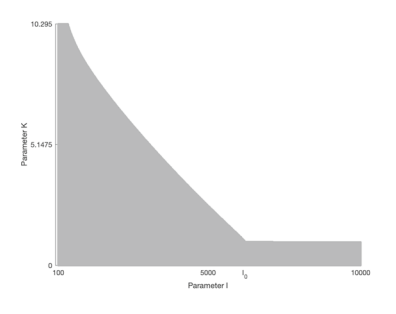
(D) Parameters $\kappa_2, \kappa_4 = 30$ is at the bottom of its range, while parameter $A_2 = 3.61$ is in the middle and $\alpha = 0.007$ is at the bottom of its range.

Fig. 3 Identifying phenotype using two dimensional projections of parameter space (I, A_{max}, α, K) . Points in the (I, K)-plane for which the pair of parameter values admits a stationary equilibrium S are grey, while points where the pair of parameters admit proliferative equilibrium P are white. Parameters from Group 2 in Table 1 are set to the bottom of their range

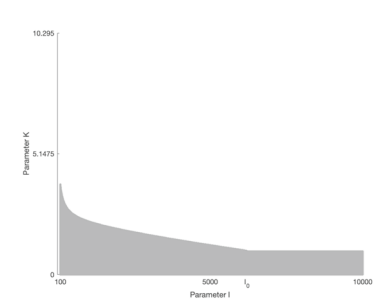
(A) and (D), which are reproduced in Fig. 5A–D. Comparing the panels in the same column shows the impact of moving the parameters in group 2 from the bottom to the middle of their range. For example, when comparing Fig. 5A–E, very little change in the qualitative behavior can be observed between the two. A similar comparison can be done with columns two, three and four of Fig. 5. Hence, we conclude that variations in the parameters in group 2 have little influence on the prevalence of S vs. P. Overall, we conclude that the effect of small changes in the group 2 parameters is much smaller than the effect of varying the parameters α , A_{max} and $\kappa_2 = \kappa_4$.



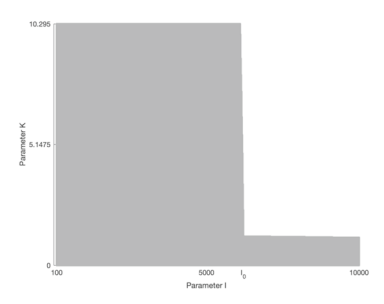
119 Page 14 of 29 J. Shea et al.



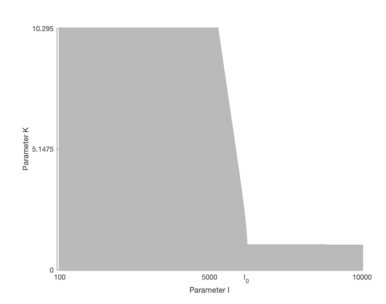
(A) Parameters $\kappa_2, \kappa_4 = 71.5$ is in the middle of its range, while $A_2 = 0.46$ is at the bottom and $\alpha = 0.3805$ is at the middle of its range.



(B) All parameters $\kappa_2, \kappa_4 = 71.5, A_2 = 3.61$ and $\alpha = 0.3805$ are at the middle of their ranges.



(C) Parameters κ_2 , $\kappa_4 = 71.5$ is at the middle of their range, while both $A_2 = 0.46$ and $\alpha = 0.007$ are at the bottom of their ranges.



(D) Parameters $\kappa_2, \kappa_4 = 71.5$ and $A_2 = 3.61$ are in the middle, while $\alpha = 0.007$ is at the bottom of its range.

Fig. 4 Identifying phenotype using two dimensional projections of parameter space (I, A_{max}, α, K) . Points in the (I, K)-plane for which the pair of parameter values admits a stationary equilibrium S are grey, while points where the pair of parameters admit proliferative equilibrium P are white. Parameters from Group 2 in Table 1 are set to the bottom of their range

4 Analysis

The model is uniformly dissipative in the non-negative orthant. Indeed, last two equations are decoupled from the first four equations and clearly dissipative. In addition,

$$\limsup_{t \to \infty} r(t) \le \frac{A}{\beta}, \qquad \limsup_{t \to \infty} m(t) \le \frac{B}{\kappa \beta}$$
 (17)



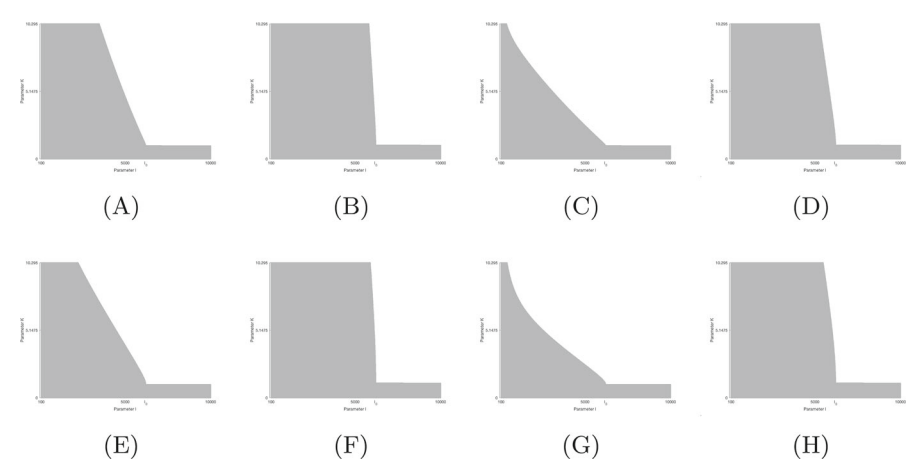


Fig. 5 Panels (A)–(D) correspond to the case where all parameters in Group 2 are set to the bottom of their range and are identical to panels (A) and (D) in Figs. 3 and 4: A Fig. 3A, B Fig. 3D, C Fig. 4A, D Fig. 4D, Panels (E)–(H) have the parameters in Group 2 set at the midpoint of their interval. Comparing panels along columns shows the impact of moving the parameters in Group 2 from the low to the middle of their range. This effect is much smaller than the effect of variations in the parameters α , A_{max} , κ_2 , κ_4

Furthermore, since

$$\dot{r}(t) + \dot{R}(t) < A - \min(\xi, \beta)(r + R),$$

then while $R + r > \frac{A}{\min(\xi, \beta)}$ then $\dot{R} + \dot{r} < 0$. Therefore

$$\limsup_{t \to \infty} (R(t) + r(t)) \le \frac{A}{\min(\xi, \beta)}$$

and therefore also

$$\limsup_{t \to \infty} R(t) \le \frac{A}{\min(\xi, \beta)}.$$
 (18)

Finally, from bound on $\limsup_{t\to\infty} m(t)$ in (17) and bound on $\limsup_{t\to\infty} R(t)$ in (18) we get that

$$\dot{p} \le KG \frac{B}{\kappa \beta} \frac{A}{\min(\xi, \beta)} - \xi p$$

and therefore

$$\limsup_{t\to\infty} p(t) \le \frac{AKGB}{\min(\xi,\beta)\kappa\beta\xi}.$$



119 Page 16 of 29 J. Shea et al.

4.1 Equilibrium Solutions

This section describes the mathematical analysis of the equilibrium solutions for the system in (10)–(15). The weak coupling of the system allows us to uniquely determine two components of the equilibrium solution for a given choice of parameters. Notice that Eq. (15) is completely decoupled from the other equations, and one can solve it explicitly for the equilibrium solution given below.

$$g^* = \frac{H}{\eta} \tag{19}$$

Substituting (19) for g in the expressions for \hat{A} and \hat{B} in (7)–(8), it follows from (14) that the value n^* solves

$$I = \gamma n(\hat{A}(n) + \hat{B}(n)). \tag{20}$$

Since both $\hat{A}(n)$ and $\hat{B}(n)$ are strictly increasing functions of n, the right hand side is a strictly increasing function of n with value zero at n = 0. This proves the following Lemma.

Lemma 2 For all parameters $s \in \mathcal{P}$ the Eq. (2) has unique positive solution n^* .

Once g^* and n^* are uniquely determined by (19) and Lemma (2), respectively, the equilibrium values of $\hat{A}(n^*, g^*)$, $\hat{B}(n^*, g^*)$ are fixed by Eqs. (7) and (8). This, in turn defines equilibrium values A^* , B^* by (9). The values n^* , g^* , A^* and B^* can be used in the Eq. (10)–(13) to compute the remaining four coordinates of the equilibria of the system (5).

4.1.1 Remaining Coordinates of the Equilibria

In order to simplify the notation we will drop the superscript * from equilibrium values of A^* and B^* . We set $\dot{r} = 0$ in (12) to obtain

$$r^* = \frac{A}{\alpha \, p^* + \beta} \tag{21}$$

Substituting this into (11) and assuming $\dot{p} = 0$, we obtain

$$GmR^* = \frac{p^*}{K} \left[\xi + \frac{\alpha A}{\alpha p^* + \beta} \right]$$
 (22)

$$R^* = \frac{1}{Gm^*} \left(\frac{p^*}{K} \right) \left[\xi + \frac{\alpha A}{\alpha p^* + \beta} \right]$$
 (23)

Setting $\dot{m} = 0$ in (13), the expression is solved for m^* as follows, where the expression for GmR^* has been replaced with (22).

$$m^* = \frac{1}{\beta} \left[f(p^*) - \frac{p^*}{\ell K} \left(\xi + \frac{\alpha A}{\alpha p^* + \beta} \right) \right]$$
 (24)



Setting $\dot{R} = 0$ in (10), we consider

$$\alpha r^* p^* = GmR^* + \xi R^* \tag{25}$$

We substitute the expressions (21), (23) and (24) into (25) to obtain a nonlinear expression for p^* .

$$\frac{\alpha A p^*}{\alpha p^* + \beta} = \frac{p^*}{K} \left(\xi + \frac{\alpha A}{\alpha p^* + \beta} \right) + \frac{\xi}{G m^*} \left(\frac{p^*}{K} \right) \left(\xi + \frac{\alpha A}{\alpha p^* + \beta} \right) \tag{26}$$

$$0 = \frac{p^*}{K} \left[\left(\xi + \frac{\alpha A}{\alpha p^* + \beta} \right) + \frac{\xi}{Gm^*} \left(\xi + \frac{\alpha A}{\alpha p^* + \beta} \right) - \frac{K\alpha A}{\alpha p^* + \beta} \right]$$
 (27)

One solution of this equation is $p^* = 0$, and there are solutions for the nonzero case as well. In the following subsections, we now consider two cases separately.

- 1. $p^* = 0$ which leads to stationary equilibrium S;
- 2. $p^* \neq 0$, which leads to proliferative equilibrium P.

4.1.2 Stationary Equilibrium S

We compute the stationary equilibrium $S = (R_0, p_0, r_0, m_0, n^*, g^*)$. Considering the case $p^* = p_0 = 0$, first note that Eq. (25) implies that if $p_0 = 0$ then $R_0 = 0$. Then from Eqs. (12), (9) and (24), we get the following sets of equilibrium values for the remaining variables.

$$r_0 := \frac{A}{\beta}$$

$$m_0 := \frac{B}{\beta \kappa} \tag{28}$$

These two components of the equilibrium solutions are fully determined by n^* and g^* , and they are as given in the previous section along with parameter choices. The stability of *S* is addressed in Sect. 5.1.

4.1.3 Proliferative Equilibrium P

We now show that for $K > K_0$ there is a unique positive equilibrium P.

Theorem 3 A unique positive equilibrium $P = (R^{\dagger}, p^{\dagger}, r^{\dagger}, m^{\dagger}, n^{*}, g^{*})$ exists, if, and only if, $K > K_0$.



119 Page 18 of 29 J. Shea et al.

Proof Using Eq. (12) components of such equilibrium satisfy

$$p = p(r) = \frac{A - \beta r}{\alpha r}. (29)$$

We note that p(r) is a strictly decreasing function or r with $p(r_0) = 0$. Observe that positive p^{\dagger} requires $A - \beta r^{\dagger} > 0$ which is equivalent to

$$r^{\dagger} < r_0. \tag{30}$$

We note that this is in agreement with the dissipativity condition (17) which also implies that

$$m^{\dagger} < m_0. \tag{31}$$

Since p(r) is decreasing, the composite function f(p(r)) in (13) is an increasing function of r with

$$f(p(r_0) = f(0) = \beta m_0 \tag{32}$$

Using (29) in Eq. (11) we get

$$GmR =: v(r), \tag{33}$$

where the function v(r) has the form

$$v(r) = \frac{p(r)}{K}(\alpha r + \xi) = \frac{1}{K}\left(1 + \frac{\xi}{\alpha r}\right)(A - \beta r).$$

A positive equilibrium r^{\dagger} must have $v(r^{\dagger}) > 0$ which is guaranteed by (30); we also note that $v(r_0) = 0$. Computing derivative

$$v'(r) = \frac{1}{K} \left[-\frac{\xi}{\alpha r^2} (A - \beta r) - \beta \left(1 + \frac{\xi}{\alpha r} \right) \right]$$

shows that under condition (30) the function v(r) is strictly decreasing. At this point of the analysis, we have expressed p=p(r) and from (33) we can express R uniquely as a function of m and r. It follows that if we show existence of unique m^{\dagger} and r^{\dagger} then we can compute $p^{\dagger}=p(r^{\dagger})$ and from (33), one obtains $R^{\dagger}=\frac{1}{Gm^{\dagger}}v(r^{\dagger})$.

To show existence of unique m^{\dagger} , r^{\dagger} , we rewrite (10) and (11), respectively, as

$$\frac{R}{p} = \frac{\alpha r}{Gm + \xi}$$
 and $\frac{R}{p} = \frac{\alpha r + \xi}{KGm}$.



Equating the right sides yields

$$\frac{Gm}{Gm + \xi} = \frac{1}{K} \left(1 + \frac{\xi}{\alpha r} \right).$$

We set

$$u(r; K) := \frac{1}{K} \left(1 + \frac{\xi}{\alpha r} \right)$$

where we emphasize the role of the parameter K. Solving for m we get

$$m = h(r; K) := \frac{\xi}{G} \frac{u(r; K)}{(1 - u(r; K))}.$$

Using straightforward differentiation it follows from $\frac{\partial u}{\partial r} < 0$ and $\frac{\partial u}{\partial K} < 0$ that

$$\frac{\partial h}{\partial r} < 0$$
 and $\frac{\partial h}{\partial K} < 0$. (34)

Observe that by definition of K_0

$$m_0 = h(r_0; K_0). (35)$$

Note that the function h(r; K) > 0 with an asymptote

$$\lim_{r \to r_h^+} h(r; K) \to \infty \tag{36}$$

with $r_b = r_b(K)$ given by solving $1 = u(r_b; K)$ which gives

$$r_b = \frac{\xi}{\alpha(K-1)}.$$

Together with (30), this implies that a relevant domain of function h(r; K) is a region $D = \{(r_b(K), r_0) \times (1, \infty)\}$. It follows from (35) and (34) that for $K < K_0$ the decreasing function $m = h(r; K) > m_0$ for all values of $r \in (r_1, r_0)$. Therefore there cannot be $m^{\dagger} = h(r^{\dagger}; K)$ with $r^{\dagger} \in (r_1, r_0)$ for $K < K_0$ satisfying condition (31). If this were the case, then one would arrive at the inequality $m^{\dagger} > m_0$, which would contradict (31).

On the other hand, when $K > K_0$ the same argument shows that $m_0 > h(r_0, K)$. In this case, we proceed as follows. Fix a value $K > K_0$. Since h(r; K) is strictly decreasing and by (36), we find the unique value of $r_1 = r_1(K)$ with $0 < r_b(K) < r_1 < r_0$ satisfying $h(r_1; K) = m_0$. Similarly, there is a unique value $m_1 = m_1(K)$ such that $m_1 := h(r_0; K)$ with $m_1 < m_0$.



119 Page 20 of 29 J. Shea et al.

We finish the argument by considering the Eq. (13). For $K > K_0$, the positive equilibria correspond to the roots of the equation

$$f(p(r)) = \frac{GmR}{\ell} + \beta m = \frac{v(r)}{\ell} + \beta h(r; K), \qquad r \in (r_1, r_0),$$

and where both functions v(r) and h(r; K), defined above, are strictly decreasing in r. Since the function f(p(r)) is increasing in r, this equation admits at most one root.

We evaluate both sides of the equation at the ends of interval (r_1, r_0) , holding K fixed. At $r = r_1$, since $r_1 < r_0$ we estimate using (32)

$$f(p(r_1)) < f(p(r_0)) = \beta m_0$$

Since $m_0 = h(r_1; K)$ and $v(r) \ge 0$ for $r \in (r_1, r_0)$ by (30) this implies

$$\beta m_0 < \frac{v(r_1)}{\ell} + \beta h(r_1; K)$$

and hence

$$f(p(r_1)) < \frac{v(r_1)}{\ell} + \beta h(r_1; K).$$

Evaluating at $r = r_0$, since $m_1 < m_0$, $v(r_0) = 0$, and $m_1 = h(r_0; K)$, we get

$$f(p(r_0)) = \beta m_0 > \beta m_1 = \frac{v(r_0)}{\ell} + \beta h(r_0; K).$$

Consequently, there is a unique intersection $(r^{\dagger}, m^{\dagger})$ between the function f(p(r)) and $\frac{v(r)}{\ell} + \beta h(r; K)$ on interval $(r_1(K), r_0)$ for all $K > K_0$. As noted earlier, the remaining coordinates $p^{\dagger} = p(r^{\dagger})$ and $R^{\dagger} = \frac{1}{Gm^{\dagger}}v(r^{\dagger})$ give unique equilibrium P for all $K > K_0$.

5 Stability of Equilibrium Solutions

The system of equations in (10)–(15) has the Jacobian matrix of the form

$$\mathbf{J}(R, p, r, m, n, g) = \begin{bmatrix} -Gm - \xi & \alpha r & \alpha p & -GR & 0 & 0 \\ KGm & -\alpha r - \xi & -\alpha p & KGR & 0 & 0 \\ 0 & -\alpha r & -\alpha p - \beta & 0 & \Phi_1 & \Phi_2 \\ -\frac{G}{\ell}m & \Psi_1 & 0 & -\frac{G}{\ell}R - \beta & \Phi_3 & \Phi_4 \\ 0 & 0 & 0 & 0 & \Phi_5 & \Phi_6 \\ 0 & 0 & 0 & 0 & 0 & -\eta \end{bmatrix}$$
(37)



where

$$\begin{split} &\Phi_{1} = \gamma_{1} A_{max} \left[\frac{\kappa_{1}}{(\kappa_{1} + n)^{2}} \right] \\ &\Phi_{2} = -\left(A_{max} \frac{n}{\kappa_{1} + n} + A_{0} \right) \frac{1}{(\kappa_{2} + g)^{2}} = -\hat{A} \gamma_{1} \\ &\Phi_{3} = \frac{1}{\kappa + p} \gamma_{2} B_{max} \left[\frac{\kappa_{3}}{(\kappa_{3} + n)^{2}} \right] \\ &\Phi_{4} = -\frac{1}{\kappa + p} \left(B_{max} \frac{n}{\kappa_{3} + n} + B_{0} \right) \frac{1}{(\kappa_{4} + g)^{2}} = -\frac{\gamma_{2}}{\kappa + p} \hat{B} \\ &\Phi_{5} = -\gamma (\hat{A} + \hat{B}) - \gamma n \left[\gamma_{1} A_{max} \frac{\kappa_{1}}{(\kappa_{1} + n)^{2}} + \gamma_{2} B_{max} \frac{\kappa_{3}}{(\kappa_{3} + n)^{2}} \right] \\ &\Phi_{6} = \gamma n \left[\left(A_{max} \frac{n}{\kappa_{1} + n} + A_{0} \right) \frac{1}{(\kappa_{2} + g)^{2}} + \left(B_{max} \frac{n}{\kappa_{3} + n} + B_{0} \right) \frac{1}{(\kappa_{4} + g)^{2}} \right] \\ &= \gamma n \left[\hat{A} \gamma_{1} + \hat{B} \gamma_{2} \right] \end{split}$$

$$\Psi_1 = \frac{-B}{(\kappa + p)^2}$$

and

$$\gamma_1 = \frac{1}{\kappa_2 + g}$$
 and $\gamma_2 = \frac{1}{\kappa_4 + g}$.

In what follows, we analyze the stability of the equilibrium solutions using the Jacobian matrix.

5.1 Stability of S

Evaluating the Jacobian matrix in (37) at the equilibrium solution S leads to

$$\mathbf{J}(S) = \begin{bmatrix} -Gm_0 - \xi & \alpha r_0 & 0 & 0 & 0 & 0 \\ KGm_0 & -\alpha r_0 - \xi & 0 & 0 & 0 & 0 \\ 0 & -\alpha r_0 & -\beta & 0 & \Phi_1 & \Phi_2 \\ -\frac{G}{\ell}m_0 & \Psi_1 & 0 & -\beta & \Phi_3 & \Phi_4 \\ 0 & 0 & 0 & 0 & \Phi_5 & \Phi_6 \\ 0 & 0 & 0 & 0 & 0 & -\eta \end{bmatrix}$$

Using the determinant expansion of J(S), four of the six eigenvalues are identified immediately as

$$\lambda_1 = -\eta$$

$$\lambda_2 = \Phi_5 < 0$$

$$\lambda_3 = -\beta$$

$$\lambda_4 = -\beta$$



119 Page 22 of 29 J. Shea et al.

and the remaining two are eigenvalues of the 2×2 matrix

$$J_2 = \begin{bmatrix} -Gm_0 - \xi & \alpha r_0 \\ KGm_0 & -\alpha r_0 - \xi \end{bmatrix}$$

which is the 2 by 2 block matrix in the upper left corner of the Jacobian matrix above. Note that the trace and determinant of this 2×2 block are given by

$$Trace(J_2) = -Gm_0 - \alpha r_0 - 2\xi < 0$$
$$Det(J_2) = (Gm_0 + \xi)(\alpha r_0 + \xi) - KG\alpha m_0 r_0.$$

When $Det(J_2) > 0$ the equilibrium S is locally asymptotically stable and when $Det(J_2) < 0$ the equilibrium is a saddle. At $Det(J_2) = 0$, stability changes in a bifurcation. The condition $Det(J_2) > 0$ is equivalent to

$$K < \frac{(Gm_0 + \xi)(\alpha r_0)}{G\alpha m_0 r_0} = \left(1 + \frac{\xi}{Gm_0}\right) \left(1 + \frac{\xi}{\alpha r_0}\right)$$
$$= \left(1 + \frac{\kappa \xi \beta}{GB}\right) \left(1 + \frac{\xi \beta}{\alpha A}\right) = \left(1 + \kappa \frac{\epsilon}{Z}\right) \left(1 + \frac{\epsilon}{X}\right)$$
$$= K_0.$$

It follows that

Lemma 4 If $K < K_0$, then S is locally asymptotically stable. If $K > K_0$, then S is a saddle.

Proof of main theorem.

We first note that the stationary equilibrium S always exists by Sect. 4.1.2. Theorem 3 proves the existence part of Theorem 1, and the stability of S is guaranteed by Lemma 4. If there are no other invariant sets but P in the interior of \mathbb{R}^{6+} , then the easy observation that the flow of the system (5) is dissipative guarantees stability of P.

6 Discussion

Growth rate of prokaryotic cells usually determines evolutionary success since higher growth rate leads to shorter time to division and hence more offspring. Since ribosomes are needed to assemble every protein in the cell, including those proteins that form the ribosome, and since ribosomes are costly for the cell to produce, ribosomal abundance control is crucial for cells to respond to changes in environmental conditions.

In this paper we develop a model of the feedback process that controls ribosome abundance. It models the concentration of ribosomes, ribosomal RNA, ribosomal proteins and their mRNA while incorporating several control mechanisms. In particular, the elongation of rrn and mRNA is influenced by the well known control molecule ppGpp, as well as the abundance of rRNA and mRNA building blocks that, in turn,



depends on abundance of cellular resources. The model presented here is a simplification of the complexity of control mechanisms in real cells. In particular, we do not consider trade-offs where cells need to commit limited resources (i.e carbon) towards transport proteins, the enzymes to process the resources and the ribosomes to build them.

In this work we analyze the equilibria of the control model. We find that the system can operate in two states: the stationary state S where there are no free ribosomes and no free ribosomal proteins; therefore, the ribosome assembly balances with its use in ribosomal protein translation and protein decay. We interpret this state as a stationary state of the cell. On the other hand at the proliferative state P, there are both free ribosomes and free ribosomal proteins, which we interpret as a state of growth for the cell, since these free ribosomes may engage in biomass growth. The transition between the equilibria depends on a relation between supply of building blocks of ribosomal proteins (aminoacids) and demand for ribosomal proteins. The supply rate is represented by K(I) where I is nutrient supply to the cell and the demand is represented by a complex expression of parameters that define the threshold K_0 . Our main result is that when the supply of building blocks for ribosomes exceeds the demand for them, the cell will have free ribosomes that are available to build protein biomass beyond ribosomes themselves.

There are three main contributions of this paper. The first is the construction of a mathematical model of a complicated biological control system. Second is the mathematical analysis of the equilibria of the six dimensional system. This analysis shows the existence of equilibria that can be readily interpreted in the biological context. Finally, we identify either parameter values or ranges of values for 23 parameters in the model, and we show that both types of equilibria exist within this set of parameters. In addition, we demonstrate that the control mechanisms indeed cause transition between the equilibria in the expected direction. An intriguing observation is that we do not find hysteresis in our model. Hysteresis is observed regularly in cellular biology as it buffers system against unexpected change of parameters caused by noise. Our model suggests that the amount of free ribosomes changes gradually as a function of nutrient supply rather than abruptly which would be expected under hysteresis.

The model developed here is clearly incomplete; even the process of ribsome assembly itself is immensely complicated (Davis and Willamson 2017). In particular, there are additional control mechanisms; only some of them are likely known. However, we hope that the model constructed and analyzed in this work and the parameters we have identified may serve as a basis for further mathematical modeling exploration of this fascinating control problem in cell biology.

Important questions, that we plan to pursue in the future, focus on how the ribosome abundance control system responds to dynamic perturbation of the resources. Cellular response to a sudden degradation of the quality or quantity of the carbon source necessitates rapid transition away from ribosome production as cells transition from exponential growth to either linear growth or simple survival. This so called *stringent* response has been studied in systems biology for quite some time 9 s Hauryliuk et al. 2015; Srivatsan and Wang 2008; Traxler et al. 2011; Boutte and Crosson 2013). Since this is a dynamical response to a shift in resource, several factors that we do not model in this work will rise in importance in future research. In particular, the fact that



119 Page 24 of 29 J. Shea et al.

transcription and translation are processes that unfold in time will require us to either model their effect by delays (Mier-y-Teran-R et al. 2010), or model them directly as transport processes (Davis et al. 2013).

Acknowledgements This research was partially supported by NSF grant DMS-1951510. We acknowledge the Indigenous nations and peoples who are the traditional owners and caretakers of the land on which this work was undertaken at Montana State University.

A Parameter Values Justification

In order to parameterize the model we use numbers for *E. coli*. There are two challenges to successful parameterization. The first is that the numbers depend on growth condition of *E. coli* so that some of the parameters (i.e. number of ribosomes in a cell) may change by two orders of magnitude. The second challenge is that our model, as every model, is a simplification and thus many parameters have to be interpreted appropriately in terms of measured data. Below is the detailed justification parameter values in Table 1.

- $\beta = 0.14 \text{ min}^{-1} = 0.00233 \text{ s}^{-1}$ Degradation rate of mRNA and rRNA. In *E. coli* mRNA lifespan is about 5 min (Milo and Phillips 2016) (BNID 106869).
- $\xi = 0.014 \text{ min}^{-1} = 0.000233 \text{ s}^{-1}$ Degradation rate of proteins. Rapidly degraded proteins in *E. coli* have lifespan about an hour or 10 times that of mRNA will do 50 minutes (Milo and Phillips 2016) (BNID 108404). Note that this constant can be also interpreted as a dilution rate of proteins due to volume growth of the cell.
- $\eta = 0.2 0.35 \text{ min}^{-1} = 0.0033 0.0058 \text{ s}^{-1} \text{ ppGpp degradation rate (Gallant et al. 1972).}$
- $\gamma = 1100$ is the number of nucleotides that are assembled into mRNA or rRNA per initiation event. Typical mRNA in *E. coli* has length 370 nm and a single nucleotide has length 0.33 nm for about 1100 nucleotides per mRNA.
- $U=1.3~\mu\mathrm{M}$ amino acid average concentration in *E. coli*. The article (Yuan et al. 2006) lists concentrations for some amino acids and they range from 0.2 μ mol/g for phenylalanine to 6.81 μ mol/g for alanine. With the conversion factor 0.36g/L we get a range $0.072-2.45~\mu\mathrm{mol/L}$ which is just $\mu\mathrm{M}$. We selected number 1.3 to be the average of this range.
- $K_m = 0.5 \,\mu\text{M}$. We chose comparable to value of U.
- $I_0=6212~\mu M$. Concentration of NTP required for balanced growth has ben measured by Buckstein et al. (2008), who cite numbers ATP = 3560 μM , CTP = 325 μM , GTP = 1660 μM , UTP = 667 μM .
- I =free parameter
- κ₂, κ₄ ∈ [30, 113] μM are half-saturation constants for ppGpp repression. During the transition from exponential to stationary phase the ppGpp concentaration is between 30 − 113 μM (Buckstein et al. 2008). We select comparable values of κ₂, κ₄.



- $\kappa_1, \kappa_3 = [10^3, 10^4] \,\mu\text{M}$ are half-concentrations of nucleotides when these become limiting. Since we derive $I_0 = 6212 \,\mu\text{M}$:concentration of NTP required for balanced growth below, we select κ_1, κ_3 to be on the same order of magnitude.
- B_2 is maximal rate of mRNA initiation in s^{-1} . Typical mRNA initiation rate is $20 \text{ min}^{-1} = 0.33 \text{s}^{-1}$ (Moran et al. 2010) (ID 111997). We will assume that the maximal rate is larger, but does not match the rate of the rrn gene and set $B_2 \in [1, 3] \text{ s}^{-1}$. Since $B_{max} = B_2 \kappa_2$, the range of B_{max} is $B_{max} \in [30, 339]$.
- $A_2 \in [0.46, 6.76] \text{ s}^{-1}$ is the maximal rate of rrn transcription initiation. There are 4-58 initiations/min/gene for rrn gene (Bremer and Dennis 1996), with 7 copies of rrn gene 28-406 initiations per min. Since $A_{max} = A_2\kappa_2$, the range of A_{max} is $A_{max} \in [13.8, 763.88]$.
- $B_0 = 0$ minimal rate of incorporation in the absence of ppGpp.
- $A_0 = 0$ minimal rate of incorporation in the absence of ppGpp.
- $\ell = 5.14$ The average size of ribosomal proteins in *E. coli* is 132 amino acids (Reuveni et al. 2017) and since each of them is encoded by 3 nt, the average length of ribosomal protein mRNA is 396 nt. On the other hand, the average spacing of ribosomes is 77 nt in *E. coli* (Siwiak and Zielenkiewicz 2013), and therefore we assume that there are $\ell = 396/77 = 5.14$ ribosomes on mRNA.

For the remainder of the parameters, we will use frequently the following numbers. All conversions to micromolar are done using Remark 5.

- Number of ribosomes per cell is 6800-72000 lower value is for slow division rate (100 min) and higher value is for fast division rate (24 min) (Moran et al. 2010) (BNID 101441). This is 11.29-119.56μM
- 2. 80% of ribosomes are actively translating (Moran et al. 2010) (BNID 102344)
- 3. There are 7 rrn genes (Condon et al. 1995). This is 0.011624 µM, see Remark 5.
- 4. The volume of *E. coli* is about 1 fL (Moran et al. 2010) (BNID 101788)
- 5. Avogadro number is $6.02214076 * 10^{23} \, mol^{-1}$.
- 6. There are 2400–7800 copies of mRNA per *E. coli* cell, depending on the growth medium (Moran et al. 2010) (BNID 112795). This is 3.98–12.95μM.
- 7. The mean initiation rate of translation in *E. coli* is about 5 initiations/min/mRNA (Moran et al. 2010) (BNID 112001), which is 0.08 initiations/sec/mRNA.

Remark 5 We describe how to convert number per cell to units of micromolar μ M. As an example we take the number of copies of rrn gene in *E. coli*, which is 7 (Condon et al. 1995). Since the volume of *E. coli* is about 1 fL (Moran et al. 2010) (BNID 101788), which is $10^{-15}L$ there are 710^{15} rrn genes per liter. Dividing by the Avogadro number $6.02214076*10^{23} \text{mol}^{-1}$ we get concentration $1.1624*10^{-8} \text{mol}/L$. Converting the units to micromolar, which is equivalent by multiplying by 10^6 we get 0.011624μ M.

- κ is Michealis-Menten constant for protein repression of its own mRNA. We computed above typical concentration of free ribosomal protein as 11.29–119.56 μ M. We assume κ belongs to the same range.
- α in units (μMs)⁻¹ is the rate of ribosome assembly from mRNA and proteins. This process is rapid requiring 2 min for production of a single ribosome (Chen et al. 2012; Lindahl 1975). There are between 11.29 119.56μM ribosomes per cell (Moran et al. 2010). Based on Chen et al. (2015) on average 1–2% of ribosomal



119 Page 26 of 29 J. Shea et al.

proteins are in the free pool, the rest is in ribosomes. So the typical size of the protein pool (these are "protein complexes" of 55 proteins) is $0.11-1.19\mu M$; the same would be true for free ribosomal RNA. We assume that

$$\alpha \in \left[\frac{1}{120}s^{-1} * \frac{1}{0.011}(\mu M)^{-1}, \frac{1}{120}s^{-1} * \frac{1}{1.19}(\mu M)^{-1}\right] = [0.007, 0.754].$$

• \hat{a} is the $1/K_D$ where K_D is the dissociation constant for binding ribosomes to ribsomal mRNA in units $(\mu \text{mol})^{-1}$. In other words,

$$\hat{a} = \frac{\text{active ribsomes on ribsomal mRNA}}{\text{free ribsomes * free ribsomal mRNA}}$$

There are between $11.29-119.56\mu M$ ribosomes per cell (Moran et al. 2010), 80% of which are actively translating (Moran et al. 2010) (BNID 102344). There are between 2400–7800 copies of mRNA per *E. coli* cell (Moran et al. 2010) (BNID 112795). Since the ribosomal protein is 9–22% of total protein, we assume that the same proportion holds for ratio between ribosomal mRNA and total mRNA. Therefore there are between 216 and 1716 ribosomal mRNA per cell which is $0.216-1.716\mu M$. If we take the lower number of ribosomes and higher number of ribosomal mRNA we get $\hat{a} = \frac{0.811.29*c}{0.211.791.716*c}$ where *c* is the proportion of ribosomal mRNA/total mRNA. This constant cancels and we get $\hat{a} = \frac{0.8}{0.21.716} = 2.33(\mu \text{mol})^{-1}$. If we take the higher number of ribosomes and lower number of ribosomal mRNA we get $\hat{a} = \frac{0.8}{0.20.216} = 18.52(\mu \text{mol})^{-1}$. Therefore

$$\hat{a} \in [2.33, 18.52].$$

- $k_2 \in [1.05, 27.18]s^{-1}$ This is K_{cat} for enzymatic reaction producing a representative ribosomal protein. The start with the number of ribosomes per cell which is 6800 to 72000 (Moran et al. 2010) (BNID 101441). We then assume that 80% or ribosomes are actively translating (Moran et al. 2010) (BNID 102344), and the elongation rate is 16 amino acids per ribosome per second. Then there are between 87, 040 and 921, 600 amino acids needed per second for protein synthesis. If we take this range and assume that 9–22% of protein in the cell are ribosomal proteins than ribosomal protein pool is created at the rate in the range [7834, 202752] amino acids/sec. Since ribosomes contain 7459 amino acids (Moran et al. 2010) (BNID 101175), the rate of production of ribosomes is 1.05–27.18 ribosomes per second. Since in our model p represents a single protein that enters ribosome with stochiometry 1, this range also represents rate of production of this representative protein, which is k_2 .
- $i_r = 0.011624 \,\mu\text{M}$ concentration of rrn genes, since there are 7 rrn genes (Condon et al. 1995). See Remark 5 for the conversion.
- i_m concentration of the ribosomal protein genes. We assume there are 55 ribosomal protein genes, one per each protein. Using conversion one gets $0.09133 \,\mu\text{M}$.



- $\omega \in [0.33, 2.64] \, \mathrm{s}^{-1}$ is the rate of formation of complex mR to produce representative ribosomal protein. We equate this number with the number of translation initiations on mRNA of that protein. The mean initiation rate of translation in E. coli is about 5 initiations/min/mRNA (Moran et al. 2010) (BNID 112001), which is 0.08 initiations/sec/mRNA. There are between 2400–7800 copies of mRNA per E. coli cell, depending on the growth medium (Moran et al. 2010) (BNID 112795). Since the ribosomal protein is 9–22% of total protein, we assume that the same proportion holds for ratio between ribosomal mRNA and total mRNA. Therefore there are between 216 and 1716 ribosomal mRNA per cell. Using these numbers as typical concentrations we estimate overall initiation to be in the range [0.08*216, 0.08*1716] = [17.28, 137.28] initiations/sec across all ribosomal mRNA in the cell. Since we model a representative ribosomal protein p, this range has to be divided by 52 which is the number of ribosomal proteins in a ribosome. This gives the range [0.33, 2.64].
- This gives the range [0.33, 2.64].

 $K = \frac{k_2}{\omega} E(I)$ where $E(I) = \frac{qI}{K_m + qI}$, see (9). K is not constant since it depends on the nutrient level I. Note that the function $E(I) \in [0, 1]$. It is also known that the lower estimate of rate k_2 and the lower estimate of ω occur at slow growth. Since both upper estimates of these rates occur at high rates, we set $K \in [0, 10.295]$ where 10.295 is the ratio of the higher estimate of k_2 and the higher estimate of ω .

References

Boutte CC, Crosson S (2013) Bacterial lifestyle shapes the regulation of stringent response activation. Trends Microbiol 21(4):174–180

Brackley CA, Romano MC, Thiel M (2010) Slow sites in an exclusion process with limited resources. Phys Rev E 82:051920. https://doi.org/10.1103/PhysRevE.82.051920

Bremer H, Dennis PP (1996) Modulation of chemical composition and other parameters of the cell by growth rate. In: Neidhardt EA (ed) Escherichia Coli and salmonella typhimurium: cellular and molecular biology. Chap. 97

Buckstein M, He J, Rubin H (2008) Characterization of nucleotide pools as a function of physiological state in Escherichia coli. J Bacteriol 190(2):718–726

Chen S, Sperling E, Silverman J, Davis J, Williamson J (2012) Measuring the dynamics of E. coli ribosome biogenesis using pulse-labeling and quantitative mass spectrometry. Mol Biosyst 8:3325–3334

Chen H, Shiroguchi K, Ge H, Xie X (2015) Genome-wide study of mRNA degradation and transcript elongation in *Escherichia coli*. Mol Syst Biol 11(781)

Condon C, French S, Squires C, Squires CL (1993) Depletion of functional ribosomal RNA operons in Escherichia coli causes increased expression of the remaining intact copies. EMBO J 12(11):4305– 4315

Condon C, Liveris D, Squires C, Schwartz I, Squires CL (1995) rRNA operon multiplicity in Escherichia coli and the physiological implications of rrn inactivation. J Bacteriol 177(14):4152–4156

Davis L, Gedeon T, Gedeon J, Thorenson J (2013) A traffic flow model for bio-polymerization processes. J Math Biol. https://doi.org/10.1007/s00285-013-0651-0

Davis J, Willamson J (2017) Structure and dynamics of bacterial ribosome biogenesis. Philos Trans B 372(20160181)

Elf J, Ehrenberg M (2005) Near-critical behavior of aminoacyl-tRNA pools in *E. coli* at rate-limiting supply of amino acids. Biophys J. 88(1): 132–146 (2005). https://doi.org/10.1529/biophysj.104.051383

Erickson DW, Schink SJ, Patsalo V, Williamson JR, Gerland U, Hwa T (2017) A global resource allocation strategy governs growth transition kinetics of Escherichia coli. Nature 551(7678):119–123

Gaal T, Bartlett MS, Ross W, Turnbough CL, Gourse RL (1997) Transcription regulation by initiating NTP concentration: rRNA synthesis in bacteria. Science 278(5346):2092–2097



119 Page 28 of 29 J. Shea et al.

Gale E, Epps H (1942) The effect of the pH of the medium during growth on the enzymic activities of bacteria (Escherichia coli and Micrococcus lysodeikticus) and the biological significance of the changes produced. Biochem J 36(7–9):600–618. https://doi.org/10.1042/bj0360600

- Gallant J, Margasin G, Finch B (1972) On the turnover of ppGpp in Escherischia coli. J Biol Chem 247(19):6055–6058
- Griffiths AJF, Gelbart WM, Miller JH, Lewontin RC (1999) Modern genetic analysis. W. H. Freeman and Co., New York
- Gyorfy Z, Draskovits G, Vernyik V, Blattner FF, Gaal T, Posfai G (2015) Engineered ribosomal RNA operon copy-number variants of *E. coli* reveal the evolutionary trade-offs shaping rRNA operon number. Nucleic Acid Res
- Hauryliuk V, Atkinson GC, Murakami KS, Tenson T, Gerdes K (2015) Recent functional insights into the role of (p)ppGpp in bacterial physiology. Nat Rev Microbiol 13:298–309
- Keener J, Sneyd J (2008) Mathematical physiology I: cellular physiology, 2nd edn. Springer, New York, NY
- Klumpp S, Hwa T (2008) Stochasticity and traffic jams in the transcription of ribosomal RNA: intriguing role of termination and antitermination. PNAS 105(47):18159–164
- Lindahl L (1975) Intermediates and time kinetics of the in vivo assembly of Escherichia coli ribosomes. J Mol Biol 92:15–37
- Michaelis L, Menten M (1913) Die kinetik der invertinwirkung. Biochem Z 49:333-369
- Mier-y-Teran-R L, Silber M, Hatzimanakatis V (2010) The origins of time-delay in template biopolymerization processes. PloS Comput Biol 6(4):1000726
- Milo R, Phillips R (2016) Biology by the numbers. Taylor & Francis LLC, New York, Garland Science Molenaar D, van Berlo R, de Ridder D, Teusink B (2009) Shifts in growth strategies reflect tradeoffs in cellular economics. Mol Syst Biol 5:323. https://doi.org/10.1038/msb.2009.82
- Moran U, Phillips R, Milo R (2010) Snapshot: key numbers in biology. Cell 141:1262-1262
- Murray HD, Schneider DA, Gourse RL (2003) Control of rRNA expression by small molecules is dynamic and nonredundant. Mol Cell 12(1):125–134. https://doi.org/10.1016/S1097-2765(03)00266-1
- Paul BJ, Ross W, Gaal T, Gourse RL (2004) rRNA transcription in Escherichia coli. Annu Rev Genet 38(1):749–770. https://doi.org/10.1146/annurev.genet.38.072902.091347. (PMID: 15568992)
- Paul BJ, Barker MM, Ross W, Schneider DA, Webb C, Foster JW, Gourse RL (2004) DksA: a critical component of the transcription initiation machinery that potentiates the regulation of rRNA promoters by ppGpp and the initiating NTP. Cell 118(3):311–322. https://doi.org/10.1016/j.cell.2004.07.009
- Reuveni S, Ehrenberg M, Paulsson J (2017) Ribosomes are optimized for autocatalytic production. Nature 547:293–297. https://doi.org/10.1038/nature22998
- Ross W, Sanchez-Vazquez P, Chen A, Lee J-H, Burgos H, Gourse R (2016) ppGpp binding to a site at the RNAP-DksA interface accounts for its dramatic effects on transcription initiation during the stringent response. Mol Cell 62(6):811–823. https://doi.org/10.1016/j.molcel.2016.04.029
- Ross W, Vrentas C, Sanchez-Vazquez P, Gaal T, Gourse R (2013) The magic spot: a ppGpp binding site on *E. coli* RNA polymerase responsible for regulation of transcription initiation. Mol Cell 50(3):420–429. https://doi.org/10.1016/j.molcel.2013.03.021
- Scott M, Gunderson CW, Mateescu EM, Zhang Z, Hwa T (2010) Interdependence of cell growth and gene expression: origins and consequences. Science 330(6007):1099–1102
- Scott M, Klumpp S, Mateescu E, Hwa T (2014) Emergence of robust growth laws from optimal regulation of ribosome synthesis. Mol Syst Biol 10(8):747
- Shaw K (2008) Negative transcription regulation in prokaryotes. Nat Educ 1(1):122
- Siwiak M, Zielenkiewicz P (2013) Transimulation protein biosynthesis web service. PLoS ONE 8(9):73943. https://doi.org/10.1371/journal.pone.0073943
- Srivatsan A, Wang JD (2008) Control of bacterial transcription, translation and replication by (p)ppGpp. Curr Opin Microbiol 11:100–15
- Traxler MF, Zacharia VM, Marquardt S, Summers SM, Nguyen H-T, Stark SE, Conway T (2011) Discretely calibrated regulatory loops controlled by ppGpp partition gene induction across the feast to famine gradient in Escherichia coli. Mol Microbiol 79(4):830–845
- Weiße AY, Oyarzún DA, Danos V, Swain PS (2015) Mechanistic links between cellular trade-offs, gene expression, and growth. Proc Natl Acad Sci 112(9):1038–1047. https://doi.org/10.1073/pnas. 1416533112



Whitford P, Geggier P, Altman R, Blanchard S, Onuchic J, Sanbonmatsu K (2010) Accommodation of aminoacyl-tRNA into the ribosome involves reversible excursions along multiple pathways. RNA 16:1196–1204

Yuan J, Fowler W, Kimball E et al (2006) Kinetic flux profiling of nitrogen assimilation in Escherichia coli. Nat Chem Biol 2:529–530

Zampieri M, Hörl M, Hotz F, et al (2019) Regulatory mechanisms underlying coordination of amino acid and glucose catabolism in *Escherichia coli*. Nat Commun **10**(3354). https://doi.org/10.1038/s41467-019-11331-5

Publisher's Note Springer Nature remains neutral with regard to jurisdictional claims in published maps and institutional affiliations.

Springer Nature or its licensor (e.g. a society or other partner) holds exclusive rights to this article under a publishing agreement with the author(s) or other rightsholder(s); author self-archiving of the accepted manuscript version of this article is solely governed by the terms of such publishing agreement and applicable law

